Monte Carlo simulation of two-dimensional hard ellipses

J. A. Cuesta* and D. Frenkel
FOM–Instituut voor Atoom- en Molecuulfysica, Kruislaan 407, 1098 SJ Amsterdam, The Netherlands
(Received 14 February 1990; revised manuscript received 23 April 1990)

We report constant-pressure Monte Carlo simulations of a system of hard ellipses with aspect ratios $k=2$, 4, and 6. The results show three different phases: isotropic, nematic, and solid, except for $k=2$, where no nematic phase is formed. In all cases the fluid-solid transition appears to be first order. However, the isotropic-nematic transition looks first order for $k=4$ and continuous, via disclination unbinding, for $k=6$. Thus a tricritical point for some k between these two values is predicted. The simulation results are also compared with a previous theoretical calculation. Satisfactory agreement is found for the equation of state, but the theoretical prediction for the location of the isotropic-nematic transition disagrees with the simulation results. Finally, we observed that the solid phase near melting exhibits anomalously large fluctuations.

I. INTRODUCTION

Since the discovery of *liquid crystals*[1] at the end of the nineteenth century, a great deal of work has been devoted to understanding the curious properties of these phases, which have structural order intermediate between that of liquids and solids. From the very beginning, the existence of these *mesophases* was known to be associated with the *anisotropic* character of the interactions between the molecules.[1] Historically, two rather different theoretical approaches have been followed to explain the stability of liquid crystals. One, due to Maier and Saupe,[2] stressed the importance of the anisotropic *attractive* interactions while the other, due to Onsager,[3] ascribed the existence of mesophases to an excluded volume effect resulting from the purely *repulsive* anistropic forces. Recent evidence, both from computer simulations[4] and from density-functional theory[5] indicates that systems of hard convex bodies may form a wide variety of liquid-crystalline phases. The nature of the mesophase depends sensitively on the shape of the molecule. One may take the point of view that these hard-core models capture the essence of liquid crystals and can be used as *reference* systems[6] in perturbative treatments of more realistic systems.

The reason for studying two-dimensional (2D) liquid-crystalline systems is twofold: first, for many practical purposes we are interested in the behavior of a thin film (of one or a few layers) of a liquid-crystalline substance (e.g., monolayers of adsorbed molecules, layers of a smectic phase, etc.), and second, from a purely theoretical point of view it is interesting to know how liquid-crystalline transitions depend on the dimensionality.

One of the main properties of most 2D systems is the lack of true *long-range order* (LRO). It is a general result of statistical mechanics[7] that $D=2$ is the lower critical dimension for which the amplitude of the fluctuations diverges logarithmically as the system size increases. As a consequence, the order parameter depends algebraically on the system size and vanishes in the thermodynamic limit. This kind of order is usually referred to as *quasi*-LRO. This property of 2D systems has been observed for the isotropic-nematic (I-N) transition both in computer simulations[8] and laboratory experiments.[9] In general, quasi-LRO is to be expected in 2D nematics if the free energy associated with collective fluctuations in the molecular orientation can be written as[1]

$$F=\tfrac{1}{2}\int K(\nabla\theta)^2 d\mathbf{r}\ , \tag{1}$$

$\theta(\mathbf{r})$ being the local molecular orientation with respect to a fixed axis and K the *renormalized Frank's constant.*[10] From this equation we can derive the logarithmic divergence of the molecular orientation fluctuations:

$$\langle\theta^2\rangle\sim\frac{k_BT}{4\pi K}\ln N\ , \tag{2}$$

with k_B the Boltzmann's constant, T the absolute temperature, and N the number of particles. As a consequence of this formula both the *order parameter* $q\equiv\langle\cos(2\theta)\rangle$ and the angular correlation functions $g_{2l}(\mathbf{r})\equiv\langle\cos\{2l[\theta(0)-\theta(r)]\}\rangle$ ($l=1,2,\ldots$) decay algebraically as

$$q\sim cN^{-k_BT/2\pi K}\ , \tag{3}$$

$$g_{2l}(r)\sim c'r^{-\eta_{2l}}\ , \tag{4}$$

with $\eta_{2l}\equiv 2l^2k_BT/\pi K$. One possible mechanism for the 2D I-N transition is through *disclination unbinding.*[11] This transition is predicted to occur at a critical value of the renormalized Frank's constant given by[8]

$$\frac{\pi K_c}{8k_BT}=1\ . \tag{5}$$

Although the I-N transition may occur through different mechanisms (for instance, a first-order phase transition) it is important to notice that *no* stable nematic phase is possible for $K<K_c$.

Among the 2D nonspherical hard-body models the simplest one is the *hard-ellipse* system. This system is characterized by the *aspect ratio* k defined by $k\equiv a/b$, a

and b being the major and the minor axis of the ellipse respectively, which is a measure for the eccentricity of the ellipses. In spite of its simplicity this system has received little attention. To our knowledge, the only theoretical results obtained thus far are those of Boublik[12] using *scaled particle theory*, the numerical solution of the *Percus-Yevick equation* by Ward and Lado,[13] and the *density-functional theory* approach for the I-N transition by Cuesta *et al.*[14] Pioneering Monte Carlo (MC) simulations of hard ellipses were reported nearly 20 years ago by Vieillard-Baron[15] (see also Ref. 8). In the present paper we report more extensive MC simulations for the hard-ellipse system.

This paper is organized as follows: In Sec. II we describe the technical details of the MC method used in the simulation. In Sec. III we report the main results of our work which are compared in Sec. IV to the existing theoretical studies concerning the I-N transition. Section V contains the main conclusions of this work.

II. COMPUTATIONAL TECHNIQUE

A. General aspects

In this section, we describe those aspects of our simulation technique that are nonstandard. For a general discussion of Monte Carlo simulations, the reader is referred to the existing literature on this subject (see, e.g., Ref. 16).

In order to facilitate comparison with existing theoretical calculations[14] of the equation of state of the hard-ellipse system, we carried out all simulations using the *constant-pressure* MC technique.[17,18] Our system contains, in most cases, approximately 200 particles in a nearly square box with periodic boundary conditions. However, in simulations of the solid phase, we do not fix the box shape but allow it to change its shape[19,20] in order to be compatible with the equilibrium shape of the unit cell of the solid phase. This is done by performing the MC sampling on the elements of the symmetrized h matrix which relates the real coordinates of the particles $\mathbf{r}_i$ to the scaled coordinates $\mathbf{s}_i$ in the following way: $\mathbf{r}_i = \mathbf{h}\cdot\mathbf{s}_i$, where the index i goes from 1 to N. In fact, we made the additional simplification of keeping $\mathbf{h}$ diagonal. In this way we can sample the *width* and *length* of the box independently.

Acceptable configurations of our system are those for which there is no overlap between any of the ellipses. A MC trial consists in moving simultaneously both the position $\mathbf{r}_i$ and the orientation $\mathbf{u}_i$ of the ith ellipse. Its $x(y)$ coordinate is changed by adding a random number $\Delta_{x(y)}$ uniformly distributed in the interval $-\Delta \le \Delta_{x(y)} \le \Delta$, and the molecular orientation, characterized by the angle θ_i, is changed by adding a random amount $\delta\theta$ uniformly distributed in the interval $-\Delta_\theta \le \delta\theta \le \Delta_\theta$. The move is rejected if the changed particle overlaps any other, and accepted otherwise. Both Δ_θ and Δ were chosen such that the overall probability of acceptance of a trial move was $\sim$20–25 %. To test the overlap between two ellipses we use the Vieillard-Baron criterion.[15]

A change in volume trial consists in multiplying by a factor $\exp(\alpha\xi)$ either the system volume V at low densities, or one of the box sides $L_{x(y)}$ randomly chosen with probability $\frac{1}{2}$, at high densities. ξ is a random number uniformly distributed in the interval $-\frac{1}{2} < \xi < \frac{1}{2}$ and α was fixed in such a way that the acceptance ratio of volume changes was $\sim$20–25 %. With this procedure we are not sampling the volume V itself but $\ln V$. This is a more convenient procedure because the reversibility of the generated Markov chain[21] is guaranteed, since the domain of the random walk in $\ln V$ coincides with the range of acceptable (positive) values of V.[22] The move is rejected if after changing the volume there is any overlap between particles and accepted with probability

$$r \equiv \min\{1, \exp[(N+1)\ln(1+\Delta V/V) - \beta P \Delta V]\}$$

otherwise,[23] where $\beta \equiv 1/k_B T$ (T, temperature and k_B Boltzmann's constant), P denotes the pressure, N is the number of particles, and $\Delta V \equiv [\exp(\alpha\xi) - 1]V$.

B. Order parameter and correlations decay

The usual nematic order parameter of a 2D N-particle system is defined as

$$q = \frac{1}{N}\left\langle \sum_{i=1}^{N} \cos(2\theta_i) \right\rangle , \tag{6}$$

where θ_i is the angle between the ith molecule and the nematic director $\mathbf{n}$. As this vector is not known *a priori* we have to use a different method to compute the order parameter. Hence we define the *tensor order parameter* Q as

$$Q_{\alpha\beta} = \frac{1}{N}\left\langle \sum_{i=1}^{N} [2u_\alpha(i)u_\beta(i) - \delta_{\alpha\beta}] \right\rangle , \tag{7}$$

where $u_\alpha(i)$ is the αth Cartesian coordinate of the unit vector specifying the orientation of molecule i. By diagonalizing the Q tensor it can be easily proven that in the thermodynamic limit its eigenvalues are $\pm q$ and its corresponding eigenvectors are the nematic director and a vector perpendicular to the latter. When the finite size of the system is taken into account, the eigenvalues of Q behave as $\pm q + O(1/\sqrt{N})$ when $q \to 0$.[24] So, even in the isotropic phase we should expect a clearly nonzero value of the computed order parameter since our system has only about 200 particles. In the nematic phase we may expect to observe quasi-LRO because we are dealing with a 2D system.[1,7] Hence, also in this phase the order parameter will exhibit a strong system-size dependence. It should be noted, that in a simulation of a finite system, the isotropic phase will resemble a nematic, once the correlation length of nematic fluctuations exceeds the size of the periodic box. In contrast, if the box size exceeds this correlation length, the eigenvalue of the Q matrix will vary as $1/\sqrt{n_d}$, where n_d is the number of nematic domains in the box.[21] In order to determine the point where the nematic phase becomes stable with respect to disclination unbinding, we must study the exponents η_{2l} of the algebraic decay of the correlation functions $g_{2l}(r)$ [see Eq. (4)] and compare them with the critical value given by (5). An analysis of the system-size dependence of the order parameter is also helpful since it can be ana-

lyzed using Eq. (3). Such an analysis allows us to estimate the point where the I-N transition takes place. It should be stressed, however, that the I-N transition in a finite system tends to occur at a somewhat lower density than in an infinite system because the computed Frank's constant in a finite system is larger than in the infinite-system limit.[21]

III. RESULTS

In order to facilitate comparison with the theoretical results of Ref. 14, simulations were performed for the same values of the aspect ratio ($k=2$, 4, and 6) that were studied in Ref. 14. In all cases the initial configuration was obtained by expanding a close-packed configuration to lower density. The fluid branch was then simulated starting from this low density. For the solid phase, we used a high-density starting configuration. The choice of the number of particles ($N=170$, 216, and 186) was dictated by the requirement that the shape of the box be almost square. Subsequent runs were started from the previous equilibrated configuration at a lower (higher) density. A typical run consisted of 10^4 steps (i.e., attempted moves per particle) for equilibration and 2×10^4 steps for analysis. We fix our reduced units by imposing $k_BT=1$ and $4ab=1$. The latter definition of length scale reduces to the definition $\sigma=1$ in the hard disk case.[25] In Table I we summarize the results of our simulations for $k=2$, 4, and 6, and in Figs. 1–3 a plot of the equation of state (in terms of the reduced pressure $P^*\equiv\pi abP/k_BT$ and the packing fraction $\eta\equiv\pi ab\rho$) is compared with the theoretical predictions of Ref. 14.

We also computed the *virial coefficients* up to B_5 using Ree and Hoover's MC method[26] and the analytical expression for B_2 derived from Boublik's formula[12] for the average excluded volume of convex bodies in $D=2$. This expression reads

$$B_2(k)/v_{\rm mol}=1+\frac{4k}{\pi^2}\left[E\left[1-\frac{1}{k^2}\right]\right]^2 \tag{8}$$

where $k=a/b$ and $E(x)=\int_0^{\pi/2}(1-x\sin^2t)^{1/2}dt$ is the complete elliptic function of the second kind. These results are summarized in Table II. A comparison between the exact B_2 [Eq. (8)] and the approximation used in Ref. 14 is made in Fig. 4. A discussion of this picture is postponed to Sec. IV. In Figs. 1–3 a plot of the five-term virial series for the equation of state is also shown. In all cases, it is found that these series fit the MC data only for very low densities. At higher densities the five-term virial series predicts a pressure that is too high. This suggests that some of the higher-order virial coefficients are negative. Below, we analyze the three cases separately.

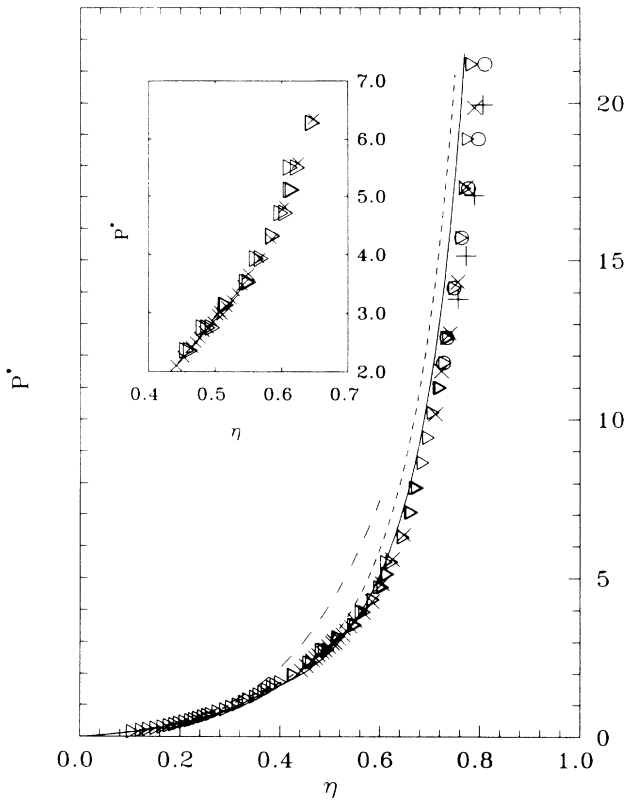

FIG. 1. Reduced pressure ($P^*\equiv\pi abP/k_BT$) as a function of the packing fraction ($\eta\equiv\pi ab\rho$) for the $k=6$ hard-ellipse system. MC simulations, compression from low density: triangles; *idem*, expansion from high density: circles; theory of Ref. 14: short-dashed line; theory with the corrected B_2: solid line; and five-term virial expansion: long-dashed line. This figure also contains the Vieillard-Baron's results[15] for the fluid branch (crosses) and the solid branch (pluses). The insert shows in more detail the region around the Vieillard-Baron's I-N transition.

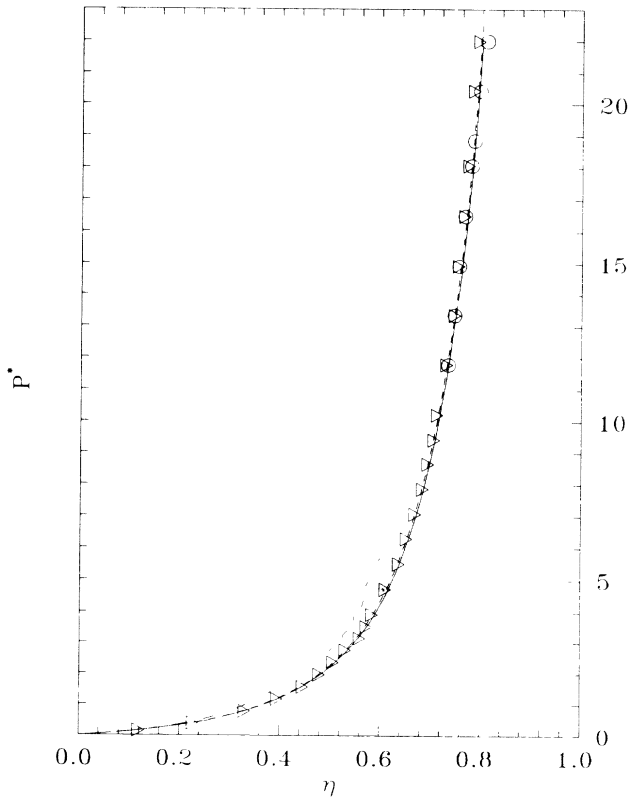

FIG. 2. The same as in Fig. 1 for the $k=2$ hard-ellipse system.

TABLE I. Equation of state data and order parameters obtained by constant-pressure Monte Carlo simulation of a system of hard ellipses with aspect ratio $k=2$, 4, and 6 ($k \equiv a/b$ with a and b the major and minor axis of the ellipses) and number of particles $N=170$, 216, and 186, respectively. The number of trial moves per particle is 2×10^4 in all cases and the overall acceptance ratio is about 20–25%. Here P stands for the pressure (units $k_BT/4ab$), ρ for the density [units $(4ab)^{-1}$] and $q \equiv \langle \cos(2\theta) \rangle$ (θ being the orientation with respect to the nematic director) for the 2D nematic order parameter. The last configuration of every run was taken to be the initial configuration of the point at a slightly higher (or lower†) pressure. The initial configuration of both the lowest and the highest points was chosen as a perfect triangular solid configuration. Notice the difference (about 2–3%) between dagged and nondagged data that indicates the existence of a first-order transition.

	$k=2$			$k=4$				$k=6$			
P	ρ	q	P	ρ	q	P	ρ	q	P	ρ	q
0.20	0.151	0.0687	0.20	0.143	0.0636	0.20	0.134	0.0713	4.50	0.701	0.638
0.50	0.288	0.0699	0.50	0.263	0.0678	0.25	0.156	0.0730	5.00	0.715	0.675
1.00	0.421	0.0721	1.00	0.379	0.0735	0.30	0.175	0.0745	5.00	0.724	0.704
1.50	0.503	0.0726	1.50	0.456	0.0824	0.35	0.194	0.0758	5.50	0.746	0.794
2.00	0.568	0.0752	2.00	0.522	0.0922	0.40	0.211	0.0782	5.50	0.748	0.789
2.50	0.610	0.0765	2.50	0.560	0.0995	0.45	0.228	0.0801	6.00	0.763	0.792
3.00	0.645	0.0741	3.00	0.608	0.0896	0.50	0.242	0.0809	6.00	0.772	0.785
3.50	0.676	0.0824	3.50	0.638	0.103	0.55	0.253	0.0832	6.50	0.781	0.748
4.00	0.713	0.0839	4.00	0.665	0.0985	0.60	0.268	0.0839	6.50	0.784	0.830
4.50	0.730	0.0804	4.50	0.691	0.168	0.65	0.281	0.0862	7.00	0.794	0.752
5.00	0.745	0.0766	5.00	0.702	0.211	0.70	0.292	0.0874	7.00	0.780	0.832
6.00	0.778	0.0819	5.50	0.724	0.149	0.75	0.302	0.0894	8.00	0.822	0.869
7.00	0.812	0.0743	6.00	0.740	0.108	0.80	0.315	0.0898	8.00	0.824	0.853
8.00	0.831	0.0788	6.50	0.766	0.198	0.85	0.325	0.0923	9.00	0.841	0.862
9.00	0.853	0.0884	7.00	0.770	0.183	0.90	0.335	0.0930	9.00	0.846	0.853
10.0	0.871	0.102	8.00	0.805	0.229	1.00	0.352	0.101	10.0	0.853	0.853
11.0	0.884	0.0908	9.00	0.820	0.117	1.10	0.371	0.100	10.0	0.853	0.853
12.0	0.899	0.121	10.0	0.840	0.229	1.20	0.386	0.108	10.0	0.860	0.847
13.0	0.907	0.0939	11.0	0.859	0.335	1.30	0.402	0.102	11.0	0.873	0.855
15.0	0.930	0.0668	12.0	0.874	0.324	1.40	0.419	0.114	12.0	0.888	0.855
17.0	0.950	0.124	13.0	0.887	0.344	1.50	0.429	0.118	13.0	0.899	0.864
19.0	0.960	0.134	14.0	0.899	0.328	1.60	0.447	0.120	13.0	0.899	0.881
21.0	0.975	0.126	15.0	0.907	0.323	1.70	0.456	0.123	14.0	0.914	0.879
23.0	0.985	0.159	16.0	0.920	0.268	1.80	0.469	0.132	14.0	0.918	0.907
26.0	0.998	0.125	17.0	0.927	0.321	1.90	0.478	0.133	15.0	0.929	0.909
28.0	1.01	0.157	18.0	0.939	0.404	2.00	0.490	0.130	16.0	0.933	0.915
†28.0	1.03	0.878	19.0	0.948	0.503	2.10	0.499	0.152	16.0	0.939	0.908
†26.0	1.01	0.757	20.0	0.957	0.528	2.20	0.511	0.153	18.0	0.954	0.929
†24.0	0.999	0.525	22.0	0.972	0.483	2.50	0.542	0.180	20.0	0.971	0.941
†23.0	0.991	0.305	24.0	0.981	0.514	2.50	0.545	0.133	22.0	0.980	0.936
†21.0	0.976	0.122	26.0	0.992	0.545	3.00	0.582	0.222	24.0	0.988	0.926
†19.0	0.961	0.091	28.0	1.00	0.588	3.00	0.589	0.175	27.0	0.998	0.937
†17.0	0.950	0.074	†28.0	1.03	0.977	3.50	0.614	0.121	†27.0	1.03	0.992
†15.0	0.935	0.077	†26.0	1.02	0.965	3.50	0.623	0.280	†24.0	1.02	0.983
			†24.0	0.998	0.932	3.50	0.632	0.387	†22.0	0.989	0.971
			†22.0	0.985	0.906	4.00	0.656	0.436	†20.0	0.972	0.956
			†20.0	0.969	0.867	4.00	0.658	0.442	†18.0	0.952	0.935
			†20.0	0.968	0.862	4.50	0.696	0.661	†16.0	0.934	0.936
			†20.0	0.966	0.860				†15.0	0.926	0.934
			†19.0	0.960	0.835						
			†18.0	0.954	0.806						
			†17.0	0.946	0.802						
			†16.0	0.941	0.821						
			†16.0	0.941	0.821						
			†15.0	0.929	0.823						
			†15.0	0.924	0.835						
			†14.0	0.909	0.759						
			†13.0	0.903	0.748						
			†12.0	0.884	0.639						
			†11.0	0.865	0.464						
			†10.0	0.851	0.470						

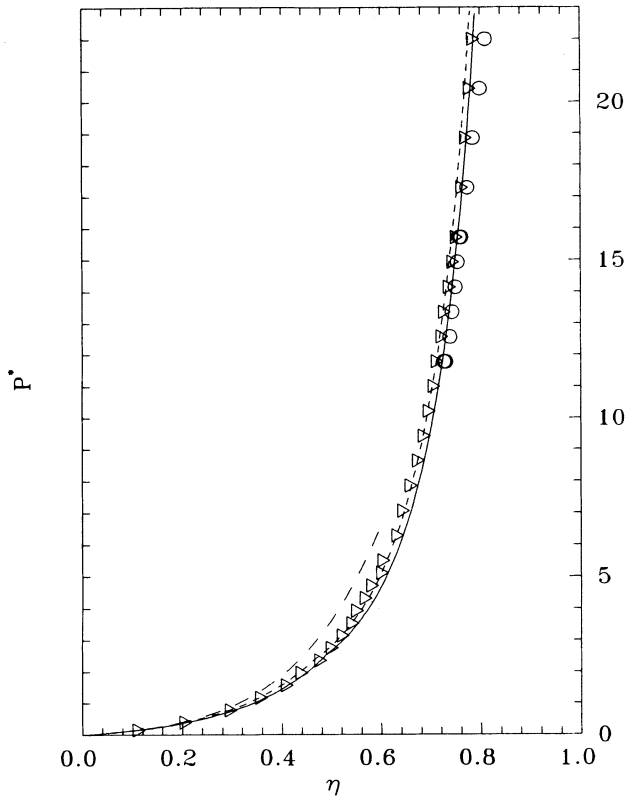

FIG. 3. The same as in Fig. 1 for the $k=4$ hard-ellipse system.

A. $k=6$ case

We first consider the aspect ratio $k=6$, i.e., the model system studied by Vieillard-Baron.[15] The results of the present simulation as well as those of Ref. 15 are plotted in Fig. 1. As it can be seen in this figure, our results and those of Vieillard-Baron fit the same curve for the equation of state. In the vicinity of $\eta\approx 0.51$, where Vieillard-Baron found a weakly first-order I-N transition, our simulation accuses strong fluctuations. Also the order-parameter plot (Fig. 5) shows that this is the region where system starts orientating. Everything suggests a possible orientational ordering transition. However, the analysis of the decay of the correlations $g_2(r)$ and $g_4(r)$ and that of the system-size behavior (see Figs. 6 and 7 and Table III) proves, according to the discussion in Sec. I, that the nematic phase can only become stable against the disclination unbinding mechanism at higher densities ($\eta\gtrsim 0.59$). This stability analysis was already made in Ref. 8 in the vicinity of the Vieillard-Baron's transition (see Table IV of that reference). In Ref. 8 the authors concluded that there was no stable nematic phase in the neighborhood of the predicted I-N phase transition. In the present simulation we extended this stability analysis up to higher densities. We find no stable nematic phase below $\eta\approx 0.59$. The reason why an apparent I-N transition is found at a lower density has already been hinted at in the previous section. As we found neither any discontinuity of the thermodynamic quantities nor evidence of

TABLE II. Virial coefficients B_3 through B_5 for the hard-ellipse system for aspect ratio $k=2$, 4, and 6, in units $(B_2)^{n-1}$. For completeness, the values for the two limits, $k=1$ († from Ref. 31 and $k=\infty$ (‡ from Ref. 8) are also reported.

k	B_3/B_2^2	B_4/B_2^3	B_5/B_2^4
1	0.7820...†	0.5322...†	0.3335...†
2	1.043(5)	1.051(2)	1.004(6)
4	0.843(0)	0.589(6)	0.330(3)
6	0.726(4)	0.371(7)	0.091(9)
∞	0.526‡	0.0180‡	−0.134‡

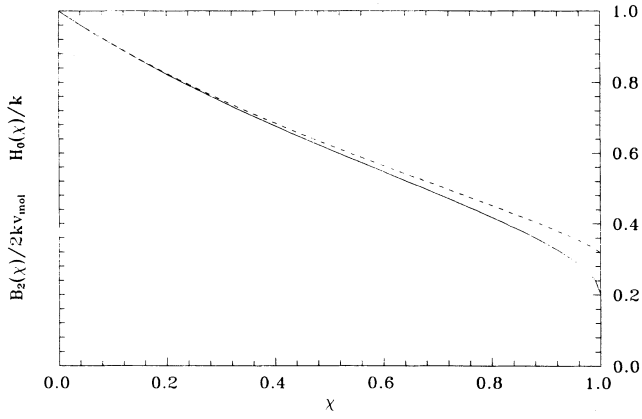

FIG. 4. Comparison between the exact second virial coefficient and the one obtained from the Gaussian-overlap approximation (see text). Solid line represents $B_2(\chi)/2kv_{\rm mol}$, with $B_2(\chi)$ given by Eq. (8), and dashed line represents $H_0(\chi)/k$, with $H_0(\chi)$ given by Eq. (10); both curves are plotted against the eccentricity $\chi\equiv(k^2-1)/(k^2+1)$, k being the aspect ratio of the ellipses. The eccentricities $[\chi(k)]$ of the three simulated cases are $\chi(2)=0.6$, $\chi(4)=0.882$, and $\chi(6)=0.946$.

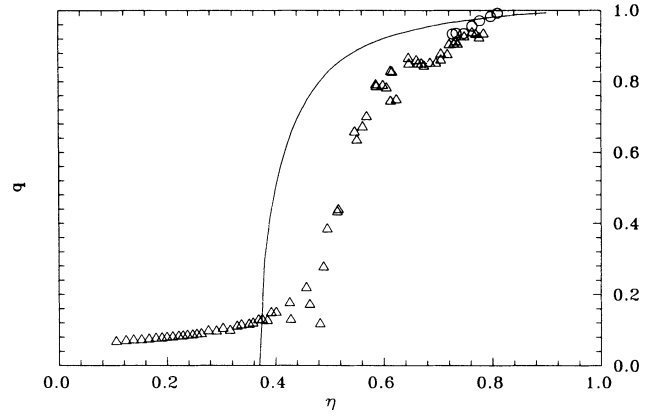

FIG. 5. Plot of the order parameter $q\equiv\langle\cos(2\theta)\rangle$ as a function of the packing fraction η for the $k=6$ hard-ellipse system. Triangles (circles) represent the MC results starting from a low (high) density, and the solid line represents the theoretical results of Ref. 14 with the corrected B_2.

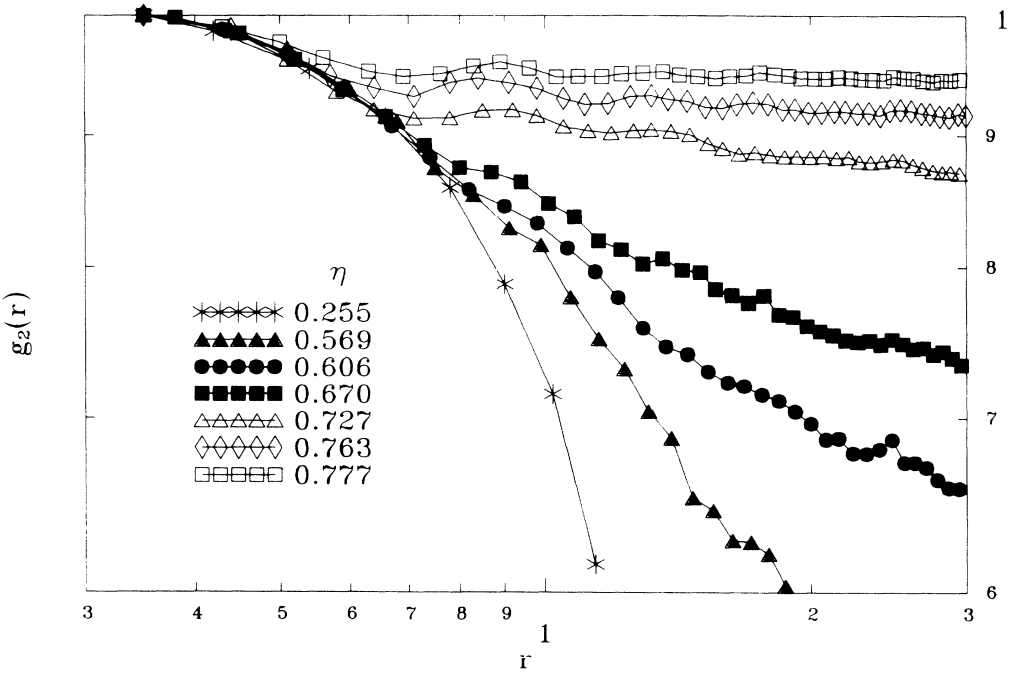

FIG. 6. Log-log plot of $g_2(r) \equiv \langle \cos\{2[\theta(0)-\theta(r)]\} \rangle$ as a function of r for the $k=6$ hard-ellipse system at several densities. Stars and solid triangles belong to the isotropic phase; solid circles, solid squares, and empty triangles belong to the nematic phase, and empty diamonds and empty squares belong to the solid phase.

hysteresis near the point where the nematic becomes stable, we conclude that for $k=6$ the *I-N* transition occurs via a *continuous* phase transition, in a way qualitatively similar to that observed for the hard needle system.[8]

At higher densities ($\eta \gtrsim 0.76$) the system exhibits a solid phase, as it can be seen in the strong peaked structure of the pair-correlation function $g_0(r)$ (see Fig. 8) as well as the snapshot of Fig. 9. The value $\eta \approx 0.76$ is only a rough estimate of the melting point obtained from the equation of state (Fig. 1); it is indeed the point below which the system is not solid anymore (strictly speaking

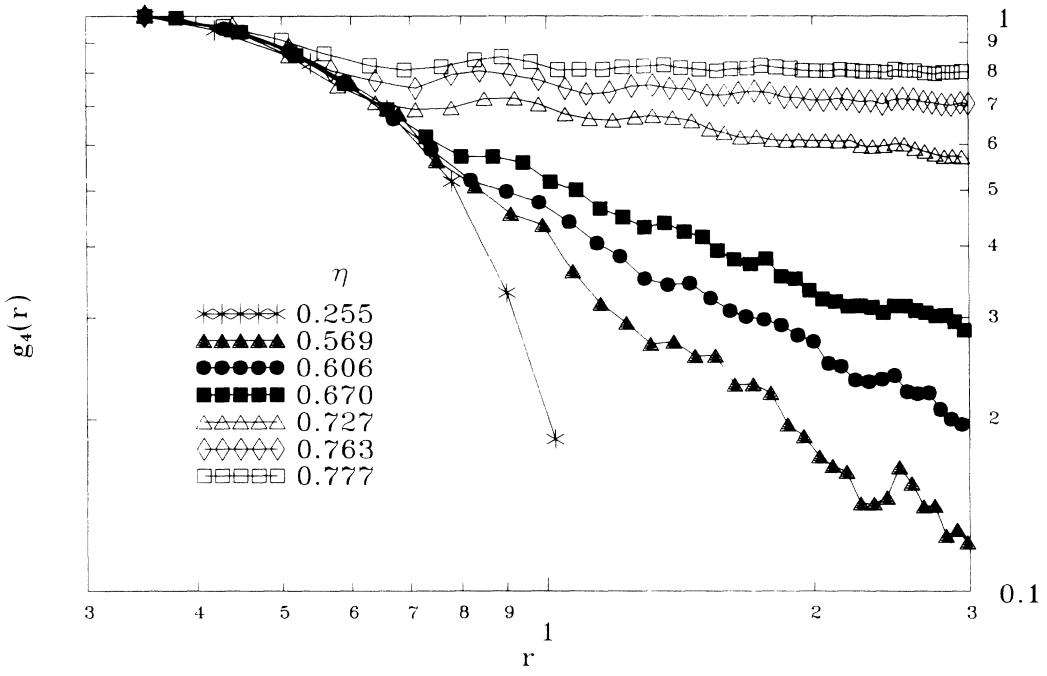

FIG. 7. The same as in Fig. 6 but for $g_4(r) \equiv \langle \cos\{4[\theta(0)-\theta(r)]\} \rangle$.

it is really a lower bound to the exact value of the melting point). Our results are very similar to those of Vieillard-Baron. The slight difference is presumably due to the different MC method used (V constant in Ref. 15, constant stress in the present work). Vieillard-Baron's estimate for the melting point ($\eta \approx 0.789$) is slightly higher than ours, which is compatible with the fact that our value is just a lower bound. In agreement with Ref. 15 we observe a *first-order* melting transition from the solid to the nematic phase. This conclusion arises from the observation of hysteresis in the plot of the equation of state[16] (see Fig. 1 and Table I): the points obtained by increasing pressure in a fluid configuration and those obtained by expanding a solid configuration do not overlap each other. On the contrary, there are two branches of the equation of state at high pressures separated by a 2–3 % density gap. We do not observe direct solid-fluid coexistence due to hysteresis effects that are typical for first-order transitions in finite periodic systems. This is why we cannot locate the melting point directly from our simulations. An accurate determination of the melting

TABLE III. Analysis of the system-size dependence of the order parameter for the $k=6$ hard-ellipse system with $N=186$ particles. The notation is chosen in such a way that $q_l \equiv \langle \cos^l(2\theta) \rangle$ stands for the lth moment of the 2D nematic order parameter averaged over the full system (1/1) and subsystems of area $\frac{1}{4}$, $\frac{1}{16}$, and $\frac{1}{64}$ of the periodic box; a_l and b_l are the parameters of the least-squares fit of all those subsystem values for q_l to the expression $\ln q_l = a_l - b_l \ln N$, where N is the average number of particles in the subsystem; r_l is the regression coefficient of this fit; c_{2l} and η_{2l} are the coefficients of the least-squares fit of the orientational correlation functions $g_2(r)$ and $g_4(r)$ ($g_{2l}(r) \equiv \langle \cos\{2l[\theta(r)-\theta(0)]\} \rangle$) to the expression $\ln g_{2l}(r) = c_{2l} - \eta_{2l} \ln r$; r_l' is the regression coefficient of this fit, and $\pi K/8k_BT$ is obtained from the expression $\langle b \rangle = k_BT/2\pi K$, where $\langle b \rangle$ is given by $\langle b \rangle = \frac{1}{5}[b_1 + (b_2/2) + (b_4/4) + (\eta_2/4) + (\eta_4/16)]$. Disclination unbinding exists for K values below the critical value given by $\pi K_c/8k_BT = 1$.

		$\eta=0.562$	$\eta=0.586$	$\eta=0.599$
q_1	$\frac{1}{1}$	0.675	0.714	0.792
	$\frac{1}{4}$	0.707	0.767	0.814
	$\frac{1}{16}$	0.773	0.820	0.856
	$\frac{1}{64}$	0.847	0.867	0.885
r_1		0.990	0.999	0.993
b_1		0.056	0.047	0.028
a_1		−0.166	−0.088	−0.092
q_2	$\frac{1}{1}$	0.461	0.515	0.628
	$\frac{1}{4}$	0.513	0.598	0.664
	$\frac{1}{16}$	0.618	0.689	0.741
	$\frac{1}{64}$	0.778	0.807	0.832
r_2		0.988	1.000	0.989
b_2		0.127	0.108	0.069
a_2		−0.144	−0.103	−0.123
q_4	$\frac{1}{1}$	0.221	0.274	0.398
	$\frac{1}{4}$	0.286	0.378	0.448
	$\frac{1}{16}$	0.421	0.504	0.568
	$\frac{1}{64}$	0.677	0.715	0.748
r_4		0.991	0.999	0.986
b_4		0.270	0.299	0.154
a_4		−0.154	−0.102	−0.161
η_2		0.345	0.252	0.145
c_2		−0.309	−0.240	−0.250
r_2'		0.996	0.996	0.989
η_4		1.426	1.174	0.658
c_4		−0.928	−0.583	−0.844
r_4'		0.976	0.988	0.990
$\pi K/8k_BT$		0.868	1.059	1.736

TABLE IV. Analysis of the system-size dependence of the order parameter for the $k=4$ hard-ellipse system with $N=216$ particles. Notation is the same as in Table III. The state point at $\eta=0.761$ was generated by expanding the solid from high densities and is a stable nematic. The point at $\eta=0.785$ was obtained by compressing the isotropic fluid. This state point is not a stable nematic. In particular, the decay of the orientational correlation functions $g_2(r)$ and $g_4(r)$ was exponential (as in the isotropic phase) instead of algebraic. Hence, we did not attempt to extract η_2 and η_4 from $g_2(r)$ and $g_4(r)$. In this case, we estimated $\langle b \rangle$ as $\langle b \rangle = \frac{1}{3}[b_1 + (b_2/2) + (b_4/4)]$.

		$\eta=0.761$	$\eta=0.785$
q_1	$\frac{1}{1}$	0.867	0.588
	$\frac{1}{4}$	0.870	0.715
	$\frac{1}{16}$	0.882	0.812
	$\frac{1}{64}$	0.929	0.913
r_1		0.889	0.992
b_1		0.016	0.104
a_1		−0.068	0.053
q_2	$\frac{1}{1}$	0.752	0.346
	$\frac{1}{4}$	0.757	0.516
	$\frac{1}{16}$	0.781	0.669
	$\frac{1}{64}$	0.870	0.845
r_2		0.895	0.991
b_2		0.034	0.212
a_2		−0.126	0.125
q_4	$\frac{1}{1}$	0.566	0.120
	$\frac{1}{4}$	0.575	0.275
	$\frac{1}{16}$	0.619	0.470
	$\frac{1}{64}$	0.774	0.744
r_4		0.906	0.990
b_4		0.073	0.434
a_4		−0.224	0.314
η_2		0.087	
c_2		−0.214	
r_2'		0.954	
η_4		0.388	
c_4		−0.790	
r_4'		0.930	
$\pi K/8k_BT$		3.289	0.590

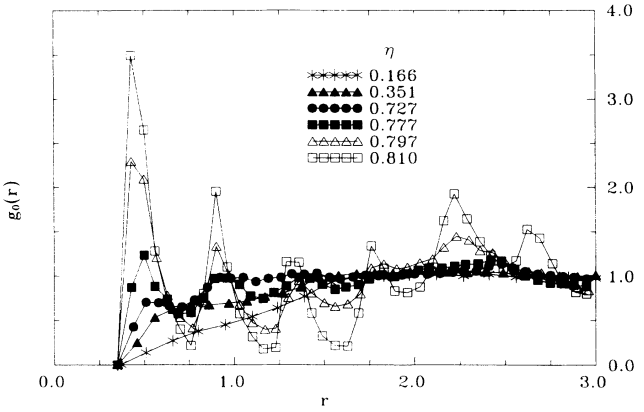

FIG. 8. Radial distribution function $g_0(r)$ as a function of r [in units $(4ab)^{1/2}$] for the $k=6$ hard-ellipse system, at several densities. Stars and solid triangles belong to the isotropic phase; solid circles belong to the nematic phase, and solid squares, empty triangles, and empty squares belong to the solid phase. Note the increasing peaked structure as η values above the freezing.

point (and the corresponding density values of the coexisting phases) would require us to compute the absolute free energy of both phases. The method has already been applied to 2D hard-core systems (hard disks[27]) and to three-dimensional (3D) hard ellipsoids of revolution.[20]

To conclude the analysis of the $k=6$ case we would like to point out that the solid phase has peculiar properties. In the snapshot of the solid phase (Fig. 9) strong anisotropic undulations can be observed. These undulations are more pronounced at long wavelengths and it seems likely that they would be even more pronounced in a larger system. In fact, it is not at all obvious that the phase observed in this figure is indeed a stable crystalline solid. Conceivably, the system behaves on a sufficiently long length scale as a 2D smectic or even as a 2D nematic. The present simulations do not permit us to test in any detail the theoretical predictions of Ostlund and Halperin[28] concerning dislocation-mediated melting of anisotropic layers. We note, however, that our observations could be compatible with the *type-I* melting scenario of Ref. 28.

B. $k=2$ case

This is the simplest case because it does not exhibit nematic phase. The system has a solid phase at densities above the value corresponding to $\eta\approx 0.78$ connected with an isotropic phase below this value (see Fig. 10) via a first-order phase transition, as it is proven by the hysteresis found in the equation of state (Fig. 2 and Table I). The order-parameter plot (Fig. 11) does not show any evidence of orientational order anywhere in between. The order parameter, q, jumps abruptly from values nearly 0 up to a very high value just at $\eta\approx 0.78$, therefore there is no *plastic* solid phase either. So, only two phases are present for this aspect ratio, connected via a first-order phase transition. However, as in the $k=6$ case, the solid phase exhibits strong fluctuations (see Fig. 10), although less pronounced than those shown in Fig. 9.

C. $k=4$ case

This is the most interesting case of our simulations since it shows a totally unexpected, qualitatively different behavior from the two previous cases. We again find

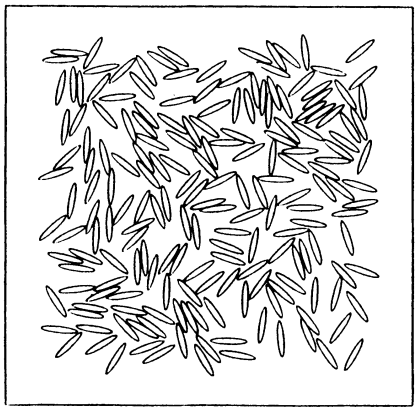

$\eta=0.329$

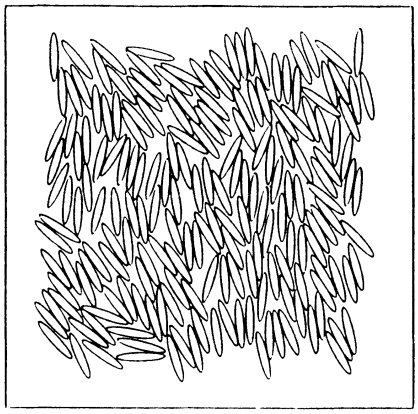

$\eta=0.599$

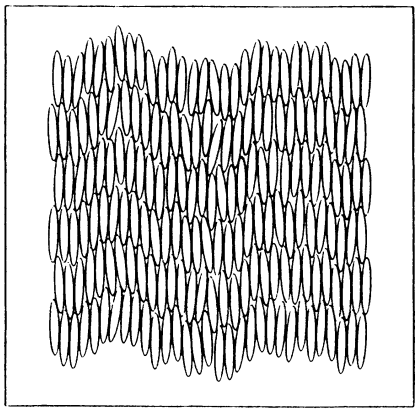

$\eta=0.809$

FIG. 9. Snapshots of the $k=6$ hard-ellipse system for the three observed phases: isotropic ($\eta=0.329$), nematic ($\eta=0.599$), and solid ($\eta=0.809$). Note that solid phase shows an anisotropic long-wavelength fluctuation (see text for details).

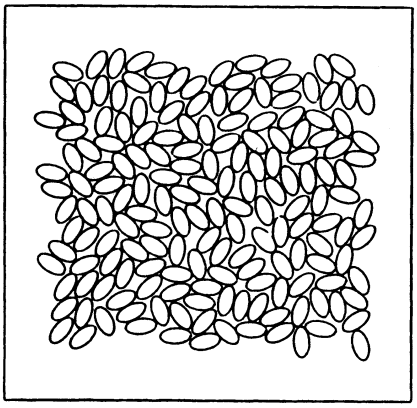

$\eta=0.712$

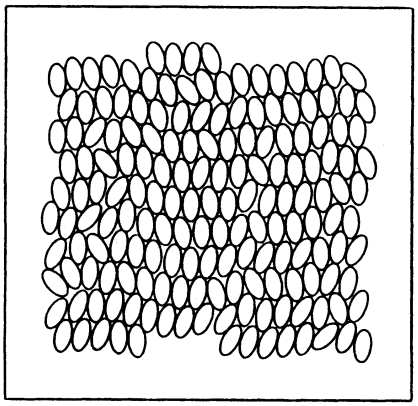

$\eta=0.810$

FIG. 10. Snapshots of the $k=2$ hard-ellipse system. The upper picture shows the isotropic phase ($\eta=0.712$) and the lower one shows the solid phase ($\eta=0.810$). No more phases were found for this case.

three phases: solid, nematic, and isotropic, but unlike the $k=6$ case, for this particular aspect ratio the system undergoes *two* first-order phase transitions (see Figs. 3 and 12 and Table I). When the pressure is increased in the isotropic phase we find that the system exhibits increasing local orientational order, but fails to form a true

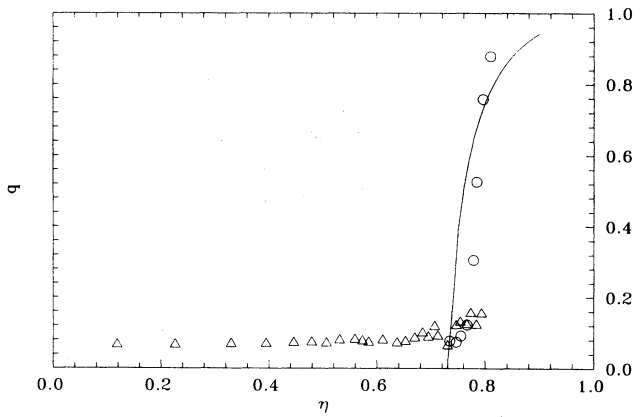

FIG. 11. The same as in Fig. 5 for the $k=2$ hard-ellipse system.

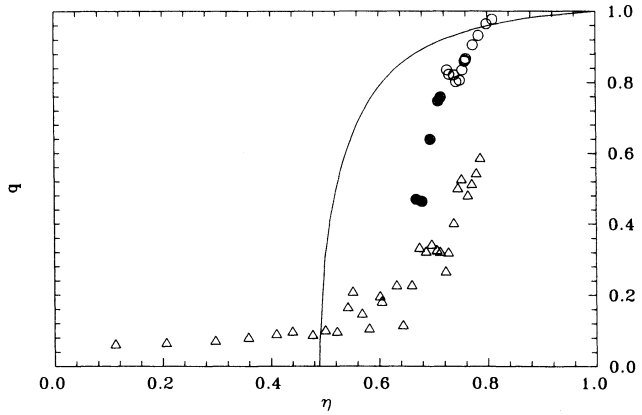

FIG. 12. The same as in Fig. 5 for the $k=4$ hard-ellipse system. Notice the noisy region around $\eta=0.75$. The filled circles below $\eta=0.75$ correspond to points that proved to be unstable in very long runs (around 3×10^6 trial moves per particle) since they fell onto the fluid branch.

nematic phase (i.e., one that is stable with respect to disclination unbinding) (see Fig. 13). When the pressure is decreased starting from the solid phase, we pass through a density range where there is a mechanically stable nematic phase (see Fig. 12 and Table IV). During this expansion, the system apparently crosses a nematic-solid (N-S) first-order transition, because recompressing from the state point at $P^*=18.8$, the solid phase cannot be

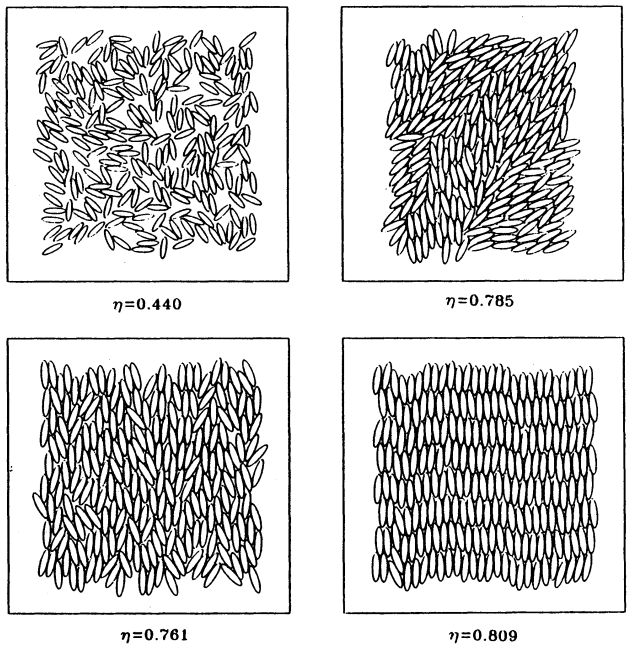

$\eta=0.440$ $\eta=0.785$

$\eta=0.761$ $\eta=0.809$

FIG. 13. Snapshots of the $k=4$ hard-ellipse system showing the isotropic phase ($\eta=0.440$), the unstable nematic ($\eta=0.785$), the stable nematic ($\eta=0.761$), and the solid phase ($\eta=0.809$). The two first pictures (isotropic and unstable nematic) were obtained by compressing the fluid whereas the two last pictures (stable nematic and solid) were obtained by expanding the solid. Notice the existence of domains in the unstable nematic.

recovered. Below this pressure the system is no longer solid, but, nevertheless, the phase shows a very high value of the orientational order parameter. Analysis of g_2 and g_4 and of the system-size dependence of the nematic order parameter (see Table IV) suggests that this nematic is stable against spontaneous disclination unbinding. At densities around $\eta \approx 0.74$ the order-parameter fluctuations become very large and below this density the order parameter decreases rapidly to values typical for the isotropic fluid branch. In longer runs all overexpanded nematic points with $\eta < 0.74$ were found to be unstable. The existence of hysteresis, the jump in the order-parameter plot and the stability of the nematic phase against disclination unbinding lead us to the conclusion that the I-N transition is first order. This result is surprising since most theories for the 2D I-N transition predict a continuous phase transition.[2,3,14] The main conclusion that can be drawn from our simulations is that there has to be a *tricritical point* somewhere in between the aspect ratios $k=4$ and 6.

IV. COMPARISON WITH DENSITY-FUNCTIONAL THEORY

In this section, we compare our computer simulation results with density-functional theory. The first density-functional theory for the I-N transition of hard ellipses was reported in Ref. 14. One of the approximations made in Ref. 14 in order to obtain an analytical expression for the direct correlation function, is the so-called Gaussian-overlap approximation (GOA) between ellipses.[29] This approximation leads to a formula for the excluded volume of two ellipses of given orientations which approaches the exact expression as eccentricity decreases. To illustrate this point the second virial coefficient obtained from the GOA is compared to the exact value given by (8) in Fig. 4. Notice the good agreement of both curves for low eccentricities and the discrepancy for high eccentricities (up to 57%, in the infinite eccentricity limit).

The fact that the density-functional theory of Ref. 14 is using an approximate second virial coefficient leads to a deviation of the theoretical equation of state from the simulated curve (a reasonable theory should guarantee at least the exact second virial coefficient). This shortcoming of the theory can easily be corrected, in a rather *ad hoc* manner, by rescaling the excluded volume by a factor

$$\lambda \equiv \frac{B_2(k)}{2v_{\mathrm{mol}}H_0(\chi)} , \tag{9}$$

with $B_2(k)$ given by (8) and $H_0(\chi)$ being the average excluded volume in the GOA:[14]

$$H_0(\chi) = \frac{2E(\chi^2)}{\pi\sqrt{1-\chi^2}} \tag{10}$$

with $E(x)$ the complete elliptic function of the second kind (introduced in the previous section) and $\chi=(1-k^2)/(1+k^2)$ (k being the aspect ratio of the ellipses). In this way we obtain an improved version of the theory of Ref. 14 in which we use the exact excluded volume for both zero and infinite[30] eccentricity limits and predict the exact value of the second virial coefficient. So, we should expect a good agreement between theory and simulations in those limits and a deviation for intermediate k values.

When comparing MC simulations with the theoretical results we distinguish two aspects of the theory: first, the success of the theory in reproducing the MC data for the equation of state, and second, the quality of its prediction for the I-N transition.

The theoretical predictions for the equation of state of hard ellipses with $k=2$, 4, and 6 are compared with the MC data in Figs. 1–3, respectively. In these figures both the prediction of the original theory of Ref. 14 and the present modification thereof are shown. In accordance with the discussion above we note that the smaller the eccentricity of the ellipses the better the theoretical curves fit the simulation points. For $k=2$ (Fig. 2) both versions of the theory coincide, and the agreement with the MC results appears to be excellent, even at high densities. Above the freezing density, the comparison has no meaning because this theory does not apply to the solid phase.[14] For $k=4$ (Fig. 3) the modified theory fits quite well both the isotropic phase at low densities and the whole nematic phase, but underestimates the pressure for intermediate values of the density in the isotropic branch. The original version of the theory reproduces the isotropic branch better but overestimates the pressure in the nematic phase. Finally, for $k=6$ (Fig. 1) both versions deviate from the experimental points as density increases, although the modified theory fits the MC data marginally better.

Whereas the density-functional theory provides a reasonable description of the equation of state of hard ellipses, it is not very successful in predicting the location of the I-N transition. First of all, it predicts a continuous phase transition for all k. There is no evidence of any tricritical point in the theory of Ref. 14 and the only effect of the present rescaling [Eq. (9)] is to shift the transition line. Moreover, the prediction of the transition points is very poor as it can be seen from the order-parameter plots (Figs. 5, 10, and 12). In Table V a comparison is

TABLE V. Location of the I-N transition points of the hard-ellipse system with $k=2$, 4, and 6. Column 1: estimate for transition density ($\eta_{I\text{-}N}^{\mathrm{Th}}$) based on the present version of the density-functional theory of Ref. 14, column 2: estimate for the transition density ($\eta_{I\text{-}N}^{\mathrm{MC}}$) based on the present MC simulations, column 3: relative deviation ($\Delta \equiv (\eta_{I\text{-}N}^{\mathrm{Th}} - \eta_{I\text{-}N}^{\mathrm{MC}})/\eta_{I\text{-}N}^{\mathrm{MC}}$ in %), and column 4: estimated melting point ($\eta_{\mathrm{Melt}}^{\mathrm{MC}}$) obtained from the present simulations. Note that we did not compute the absolute free energy of all phases involved. Therefore our estimate of the location of all first-order transitions is not very accurate.

k	$\eta_{I\text{-}N}^{\mathrm{Th}}$	$\eta_{I\text{-}N}^{\mathrm{MC}}$	Δ(%)	$\eta_{\mathrm{Melt}}^{\mathrm{MC}}$
2	0.74			$\gtrsim 0.78$
4	0.49	~ 0.74	34	$\gtrsim 0.79$
6	0.38	~ 0.59	36	$\gtrsim 0.76$

made between the I-N transition points predicted by the present version of the density-functional theory and the simulations (the original theory[14] does even worse).

We think the main reason for this failure of the theory is the mean-field character of the involved approximations. In Ref. 14 an *effective* density is found to account for the effect of the nematic ordering on the direct correlation function. With such approximation it is clear that the strong influence of the fluctuations, which are responsible for the peculiar behavior of ordering in 2D systems, is not considered at all, and then, only qualitative agreement with simulations is to be expected in this matter.

V. CONCLUSIONS

In this paper we have reported results of a MC simulation of the hard-ellipse system for three values of the aspect ratio $k=2$, 4, and 6. The simulation data indicate that there exist four phases: isotropic, nematic, solid, and plastic (the latter was observed by Vieillard-Baron[15] for very low k, but was not observed by us for $k \geq 2$); the melting transition appears to be first order and the I-N transition, which is only present for $k > 2$, is first order for $k=4$ and continuous, via disclination unbinding, for $k=6$. An important result of our work is that there must exist a tricritical point on the I-N transition line somewhere between $k=4$ and 6. We have not observed any direct evidence for the existence of a 2D smectic phase in our simulations. However, we cannot rule out the possibility that for much larger system sizes, our "solid" phase will, in fact, turn out to be a 2D "smectic" (in the sense defined by Ostlund and Halperin[28]).

We have also compared our data with the existing theoretical results for the I-N transition.[14] We find that the best density-functional theory that is presently available reproduces the simulated equation of state reasonably well, but fails to predict the correct transition density. More seriously, the present theory does not reproduce the nature of the 2D I-N transition correctly.

ACKNOWLEDGMENTS

The work of the Fundamenteel Onderzoek der Materie (FOM) Institute is part of the research program of FOM and is supported by the Nederlandse Organisatie voor Wetenschappelijk Onderzoek (NWO). This work has also been partly sponsored by the Dirección General de Investigación Científica y Técnica (DGICYT) (Spain) Grant PB88-0140. One of us (J.A.C.) thanks M. Baus for many useful discussions and a critical reading of the manuscript, C. F. Tejero for his comments, A. Sanchez and R. Brito for suggestions, and in particular all the people at Atoom-en Molecuulfysica (AMOLF) for their hospitality.

*Permanent address: Física Aplicada I, Facultad de Ciencias Físicas, Universidad Complutense de Madrid, 28040-Madrid, Spain.

[1]P. G. De Gennes, *The Physics of Liquid Crystals* (Clarendon, Oxford, 1974).

[2]W. Maier and A. Saupe, Z. Naturforsch. Teil A **13**, 564 (1958); **14**, 882 (1959); **15**, 287 (1960).

[3]L. Onsager, Ann. N. Y. Sci. **51**, 627 (1949).

[4]For a review see D. Frenkel, J. Phys. Chem. **92**, 3280 (1988).

[5]B. H. Mulder and D. Frenkel, Mol. Phys. **55**, 1193 (1985); U. P. Singh and Y. Singh, Phys. Rev. A **33**, 2725 (1986); M. Baus, J. L. Colot, X. G. Wu, and H. Xu, Phys. Rev. Lett. **59**, 2184 (1987); J. L. Colot, X. G. Wu, H. Xu, and M. Baus, Phys. Rev. A **38**, 2022 (1988); A. M. Somoza and P. Tarazona, Phys. Rev. Lett. **61**, 2566 (1988).

[6]J. P. Hansen and I. R. McDonald, *Theory of Simple Liquids* (Academic, London, 1976); D. A. McQuarrie, *Statistical Mechanics* (Harper and Row, New York, 1976).

[7]L. Landau and E. Lifshitz, *Statistical Physics* (Pergamon, Oxford, 1959).

[8]D. Frenkel and R. Eppenga, Phys. Rev. A **31**, 1776 (1985).

[9]D. H. van Winkle and N. A. Clark, Phys. Rev. A **38**, 1573 (1988).

[10]D. R. Nelson and R. A. Pelcovits, Phys. Rev. B **16**, 2191 (1977).

[11]J. M. Kosterlitz and D. J. Thouless, J. Phys. C **6**, 1181 (1973).

[12]T. Boublik, Mol. Phys. **29**, 421 (1975).

[13]D. A. Ward and F. Lado, Mol. Phys. **63**, 623 (1988).

[14]J. A. Cuesta, C. F. Tejero, and M. Baus, Phys. Rev. A **39**, 6498 (1989).

[15]J. Vieillard-Baron, J. Chem. Phys. **56**, 4729 (1972).

[16]M. H. Kalos and P. A. Withlock, *Monte Carlo Methods* (Wiley, New York, 1986); M. P. Allen and D. J. Tildesley, *Computer Simulation of Liquids* (Clarendon, Oxford, 1987).

[17]W. W. Wood, J. Chem. Phys. **48**, 415 (1968).

[18]I. R. McDonald, Mol. Phys. **23**, 41 (1972).

[19]M. Parrinello and A. Rahman, Phys. Rev. Lett. **45**, 1196 (1980).

[20]D. Frenkel and B. M. Mulder, Mol. Phys. **55**, 1171 (1985).

[21]R. Eppenga and D. Frenkel, Mol. Phys. **52**, 1303 (1984).

[22]Notice that if we had changed V by adding an amount ΔV as we did for the positions and orientations, the range of possible values of V would contain also the negative ones, which have no physical meaning.

[23]The following point is worth pointing out: at first sight, it looks as if the only possibility to get overlap between convex particles is by decreasing volume. This is only true if we change the volume but not the box shape. However, if we vary the length and width of the periodic box independently, then there are some configurations that will produce an overlap between particles by increasing volume (provided that the molecules are sufficiently anisometric).

[24]We can estimate this finite-size effect following the argument in the Appendix of Ref. 21.

[25]B. J. Alder and T. E. Wainwright, Phys. Rev. **127**, 359 (1962).

[26]F. H. Ree and W. G. Hoover, J. Chem. Phys. **40**, 939 (1963).

[27]W. G. Hoover and F. H. Ree, J. Chem. Phys. **47**, 4873 (1967).

[28]S. Ostlund and B. I. Halperin, Phys. Rev. B **23**, 335 (1981).

[29]B. J. Berne and P. Pechukas, J. Chem. Phys. **56**, 4213 (1972).

[30]In the $k \to \infty$ limit this improvement of the theory was already performed in Ref. 14 since the functional form for the excluded volume in this limit is equivalent to that of the hard needle system except a constant factor; to compare to the simulation results of Ref. 8 the second virial coefficient was then rescaled so as to reproduce the exact value. The agreement between theory and simulations obtained in this way was very good.

[31]M. Baus and J. L. Colot, Phys. Rev. A **36**, 3912 (1987).